

## Research Article

# Stability Analysis of Water-Resistant Strata in Karst Tunnel Based on Releasable Elastic Strain Energy

**Qin Liu,<sup>1,2</sup> Lai Wei,<sup>1</sup> Jianxun Chen,<sup>2</sup> Yanbin Luo,<sup>2</sup> Pei Huang,<sup>1</sup>  
Hongyu Wang,<sup>2</sup> and Jiaqi Guo<sup>3</sup>**

<sup>1</sup>*School of Civil Engineering, Chang'an University, Xi'an 710064, China*

<sup>2</sup>*School of Highway, Chang'an University, Xi'an 710064, China*

<sup>3</sup>*School of Civil Engineering, Henan Polytechnic University, Jiaozuo 454000, China*

Correspondence should be addressed to Qin Liu; chinlau@qq.com and Jianxun Chen; chenjx1969@163.com

Received 2 November 2016; Accepted 22 January 2017; Published 2 March 2017

Academic Editor: Sergii V. Kavun

Copyright © 2017 Qin Liu et al. This is an open access article distributed under the Creative Commons Attribution License, which permits unrestricted use, distribution, and reproduction in any medium, provided the original work is properly cited.

In this paper, the energy instability criterion of water-resistant strata and rock mass failure index (RMFI) are proposed, respectively, based on releasable elastic strain energy  $U^e$ . RMFI is employed to represent the damage extent of water-resistant strata. When  $RMFI < 1.0$ , rock mass is stable. When  $RMFI = 1.0$ , rock mass is in the critical instability state. When  $RMFI > 1.0$ , rock mass is unstable. The releasable elastic strain energy  $U^e$  and RMFI program is performed by FISH programming language of Flac<sup>3D</sup> software. Then, the authors apply Flac<sup>3D</sup> software to analyze the distribution law of releasable elastic strain energy  $U^e$  and failure zone under different width of concealed karst cave. Finally, combined with the numerical analysis, a case study is carried out to illustrate the rationality, effectiveness, and feasibility through using RMFI to predict safe thickness of water-resistant strata.

## 1. Introduction

In practical engineering, most water inrush and mud burst disaster in karst tunnel is caused by insufficient safety thickness of water-resistant strata between concealed karst cave and tunnel [1–3]. Thus, during the karst tunnel construction, it is of important engineering significance to determine the thickness of water-resistant strata rationally. For example, when we adopt “energy-releasing and pressure-reducing” method to address the karst cavity filled with water, a certain thickness of rock plug is required to prevent rock plug from being crushed, and that can cause water inrush disaster. In addition, during the karst tunnel construction, we need to change construction procedure and determine reasonable safe distance when closing to the small and medium filling type karst cave. Generally, if the thickness of water-resistant strata, which is determined by a water-resistant strata stability criterion, is too small, the difficulty of engineering treatment and cost will decrease. Nevertheless, it increases the instability probability of water-resistant strata. On the contrary,

if the thickness of water-resistant strata is too large, it will cause unnecessary economic waste obviously. Moreover, it is impossible to relocate the tunnel. Thus it can be seen that selecting reasonable stability criterion of water-resistant strata to determine the thickness is directly related to the tunnel design, construction, and operation safety.

At present, simplified mechanical model and numerical simulation are adopted to analyze the stability of water-resistant strata and determine the thickness. Generally, water-resistant strata are simplified as a mechanical calculation model of beam and slab [4–8], and the calculation is simple and clear. However, it is of limited use without considering the influence factors of karst tunnel stability. Numerical simulation can be employed to evaluate the stability of water-resistant strata with considering the influence factors. Generally speaking, the plastic zone size is used to estimate the stability of water-resistant strata [2–10]. In fact, the occurrence of plastic zone in rock mass does not mean that failure occurs in rock mass. Only when the equivalent plastic strain reaches a certain value, failure will occur in rock mass [11],

and the plastic zone is only given as a range, which is single information. The information, such as the rock mass damage degree in plastic zone, the most likely damaged area, and the evolution law of damage degree, is very difficult to obtain through single index of plastic zone size [12]. On the whole, the plastic zone is intuitive but not objective.

It can be seen from the law of thermodynamics that energy conversion is the essential characteristics of material physical process, and the material damage is a kind of state instability under energy drive. During the whole process from stress to failure, rock mass exchanges energy with surrounding rock all the time. Therefore, it is more conducive to reflect the essential characteristics of karst tunnel rock mass global failure through researching energy change law during deformation and failure process of karst limestone and the instability criterion of water-resistant strata based on releasable elastic strain energy. In the aspects of energy principle of rock mass stability, many scholars have carried out some researches and achieved a lot of results [12–19]. However, most researches focus on rock burst prediction in mining engineering, which can provide train of thought for stability analysis of karst tunnel based on releasable elastic strain energy. Currently, energy principle is seldom applied in stability analysis of karst tunnel. So we tried to introduce the energy principle into the stability analysis of rock mass excavated in karst area, embedding the energy principle-based failure criterion in finite element or finite difference software, which is of practical interest to ensure the stability of water-resistant strata. Thus, it has important engineering application value that energy principle is employed to analyze the stability of water-resistant strata. If the instability criterion program of water-resistant strata based on releasable elastic strain energy is embedded into the numerical analysis software, it can not only get the scope of the damage zone, but also obtain the damage degree and the change law of each point. Overall, the safety thickness of the water-resistant strata is determined though analyzing the stability of the karst tunnel based on the releasable elastic strain energy, which is of great theoretical significance and engineering application value in guiding the design and construction, preventing the tunnel water inrush and mud burst disaster and ensuring the construction safety.

## 2. Instability Criterion of Water-Resistant Strata Based on Releasable Elastic Strain Energy

**2.1. Calculation of Releasable Elastic Strain Energy of Rock Mass.** Taking unit volume of the rock mass unit for energy analysis, it can be seen from the law of conservation of energy

$$W = U = U^e + U^d, \quad (1)$$

where  $W$  is the work done by the outside to the rock, and  $U$  is the total energy of the rock absorbed from outside.  $U^e$  is the releasable elastic strain energy.  $U^d$  is the dissipation energy. The relationship between  $U^e$  and  $U^d$  is shown in Figure 1.

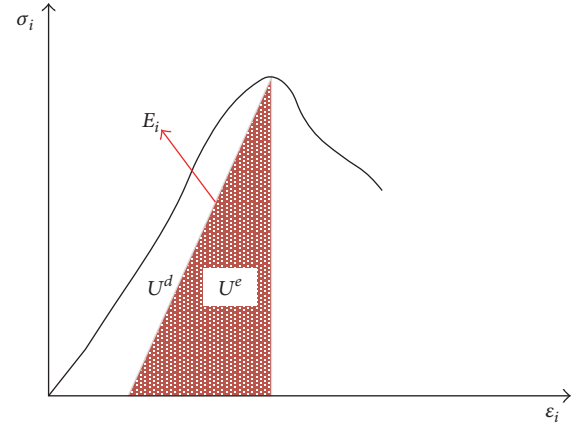


FIGURE 1: Calculation schematic of  $U^d$  and  $U^e$  in  $i$  direction.

In the shaded area,  $U^e$  refers to the releasable elastic strain energy, and  $U^d$  refers to the dissipation energy, which mainly includes internal damage energy and plastic strain energy.

$$\begin{aligned} U &= \int_0^{\epsilon_i} \sigma_i d\epsilon_i \quad (i = 1, 2, 3) \\ U^e &= \int_0^{\epsilon_i^e} \sigma_i d\epsilon_i^e \quad (i = 1, 2, 3) \\ \epsilon_i^e &= \frac{1}{E_i} [\sigma_i - \mu_i (\sigma_j + \sigma_k)] \quad (i = 1, 2, 3), \end{aligned} \quad (2)$$

where  $\sigma_i$  ( $i = 1, 2, 3$ ) is principal stress in three directions.  $\epsilon_i$  ( $i = 1, 2, 3$ ) is the total strain in three directions.  $\epsilon_i^e$  is elastic strain in three directions.  $\sigma_i, \sigma_j, \sigma_k$  ( $i, j, k = 1, 2, 3$ ) are principal stresses.  $\mu_i$  is Poisson's ratio.  $E_i$  is the unloaded elastic modulus in three directions. Assuming  $\mu_i$  is not affected by damage, denoted by  $\mu$ , we can gain

$$\begin{aligned} U^e &= \frac{1}{2} \left\{ \frac{\sigma_1^2}{E_1} + \frac{\sigma_2^2}{E_2} + \frac{\sigma_3^2}{E_3} - \mu \left[ \left( \frac{1}{E_1} + \frac{1}{E_2} \right) \sigma_1 \sigma_2 \right. \right. \\ &\quad \left. \left. + \left( \frac{1}{E_2} + \frac{1}{E_3} \right) \sigma_2 \sigma_3 + \left( \frac{1}{E_1} + \frac{1}{E_3} \right) \sigma_1 \sigma_3 \right] \right\}. \end{aligned} \quad (3)$$

In order to simplify the calculation, the initial elastic modulus  $E_0$  is taken instead of  $E_i$  usually. So (3) can be rewritten as [14]

$$\begin{aligned} U^e &= \frac{1}{2E_0} \\ &\cdot [\sigma_1^2 + \sigma_2^2 + \sigma_3^2 - 2\mu (\sigma_1 \sigma_2 + \sigma_2 \sigma_3 + \sigma_1 \sigma_3)]. \end{aligned} \quad (4)$$

**2.2. Establishment of RMFI (Rock Mass Failure Index) Based on Releasable Elastic Strain Energy.** Most of the energy input to the rock mass from outside is transformed to the releasable elastic strain energy  $U^e$  and stored in the rock mass. When the releasable elastic strain energy  $U^e$  reaches the surface energy  $U^0$  of the rock mass unit, global failure will occur. It should be noted that the releasable elastic strain energy  $U^e$  is most likely

to be released in the direction of the minor principal stress  $\sigma_3$  [14]. In order to unify symbols, we set the compressive stress as positive and the tensile stress as negative in this paper. Academician Xie et al. give the global failure criterion of rock mass unit [14], which is elaborated as follows.

**2.2.1. Global Failure Criterion of Rock Mass Unit under Triaxial Compression.** Most engineering rock mass units are in triaxial compression state ( $\sigma_1 > \sigma_2 > \sigma_3 \geq 0$ ). The releasable elastic strain energy is easy to release in the direction of  $\sigma_3$ , which is easy to release along the direction of the main stress difference  $\sigma_1 - \sigma_3$  and is proportional to the relationship between  $\sigma_1 - \sigma_i$ . If the strain energy release rate in the  $i$  direction is defined as  $R_i$ , then

$$R_i = K_i (\sigma_1 - \sigma_i) U^e \quad (i = 1, 2, 3), \quad (5)$$

where  $K_i$  is the material constant. The maximum energy release rate occurs in the direction of the minimum compressive stress; then  $R_3 = K_3 (\sigma_1 - \sigma_3) U^e$ . When the maximum strain energy release rate  $R_3$  exceeds the critical release rate  $R_c$ , the releasable elastic strain energy  $U^e$  which is stored in the rock mass unit is released in this direction first. When the releasable elastic strain energy  $U^e$  of the rock mass unit reaches the surface energy  $U^0$  required for the global failure of the rock mass unit, the global failure of the rock mass will occur. Then it satisfies

$$R_3 = K_3 (\sigma_1 - \sigma_3) U^e = R_c, \quad (6)$$

where  $U^e$  is the releasable elastic strain energy of rock mass, which is determined by (4).  $R_c$  is the material constant, which can be determined by uniaxial compression test.

In the uniaxial compression test,  $\sigma_1 = \sigma_c$ ,  $\sigma_2 = \sigma_3 = 0$ , from (4), we can gain

$$U^e = \frac{\sigma_c^2}{2E_0}. \quad (7)$$

Substituting (7) into (6), one obtains

$$R_c = K_3 \frac{\sigma_c^3}{2E_0}. \quad (8)$$

Substituting (8) into (6), eliminating  $K_3$ , one obtains

$$(\sigma_1 - \sigma_3) U^e = \frac{\sigma_c^3}{2E_0}. \quad (9)$$

Substituting (4) into (9), one obtains

$$\begin{aligned} & [\sigma_1^2 + \sigma_2^2 + \sigma_3^2 - 2\mu(\sigma_1\sigma_2 + \sigma_2\sigma_3 + \sigma_1\sigma_3)] \\ & \cdot (\sigma_1 - \sigma_3) = \sigma_c^3. \end{aligned} \quad (10)$$

Equation (10) [14] is the global failure criterion of the rock mass unit in the triaxial compression state.

**2.2.2. Global Failure Criterion of Rock Mass Unit under Tension at Least in One Direction.** Tensile stress often appears in engineering rock mass, such as unloading rock mass. It represents a kind of situation that the global failure is prone to occur. When the rock mass unit is under tension state at least in one direction ( $\sigma_3 < 0$ ), because the tensile stress in any direction will promote the release of the releasable elastic strain energy, the strain energy release rate  $R_i$  is distributed according to the value of the principal stress, and then

$$R_i = K_i \sigma_i U^e \quad (i = 1, 2, 3). \quad (11)$$

The maximum strain energy release rate occurs in the direction of maximum tensile stress. When the failure occurs in rock mass, it meets the following requirements:

$$R_3 = K_3 \sigma_3 U^e = R_t, \quad (12)$$

where  $U^e$  is the releasable elastic strain energy of rock mass, which is determined by (4).  $R_t$  is the material constant, which can be determined by uniaxial compression test.

In the uniaxial compression test,  $\sigma_3 = \sigma_t$ ,  $\sigma_1 = \sigma_2 = 0$ , from (4), we can gain

$$U^e = \frac{\sigma_t^2}{2E_0}. \quad (13)$$

Substituting (4) into (12), one obtains

$$R_t = K_3 \frac{\sigma_t^3}{2E_0}. \quad (14)$$

Substituting (14) into (12), eliminating  $K_3$ , one obtains

$$\sigma_3 U^e = \frac{\sigma_t^3}{2E_0}. \quad (15)$$

Substituting (4) into (15), one obtains

$$\sigma_3 [\sigma_1^2 + \sigma_2^2 + \sigma_3^2 - 2\mu(\sigma_1\sigma_2 + \sigma_2\sigma_3 + \sigma_1\sigma_3)] = \sigma_t^3. \quad (16)$$

Equation (16) [14] is the global failure criterion of the rock mass unit under tension at least in one direction.

**2.2.3. Establishment of RMFI (Rock Mass Failure Index).** When formulas (10) and (16) are employed to evaluate the stability of engineering rock mass,  $\sigma_t$  is tensile strength of rock mass  $\sigma_{tm}$  (negative values), and  $\sigma_c$  is uniaxial compressive strength of rock mass  $\sigma_{cm}$  (positive value). We define the damage degree of rock mass as RMFI (rock mass failure index) in this paper which is given by

RMFI

$$= \frac{(\sigma_1 - \sigma_3) [\sigma_1^2 + \sigma_2^2 + \sigma_3^2 - 2\mu(\sigma_1\sigma_2 + \sigma_2\sigma_3 + \sigma_1\sigma_3)]}{\sigma_{cm}^3} \quad (\sigma_3 > 0) \quad (17)$$

$$\text{RMFI} = \frac{\sigma_3 [\sigma_1^2 + \sigma_2^2 + \sigma_3^2 - 2\mu(\sigma_1\sigma_2 + \sigma_2\sigma_3 + \sigma_1\sigma_3)]}{\sigma_{tm}^3} \quad (\sigma_3 < 0).$$

TABLE 1: Mechanical parameters of rock mass.

Internal friction angle/(°)	Cohesion/MPa	Deformation modulus/GPa	Compression strength/MPa	Tensile strength/MPa	Bulk modulus/GPa	Shear modulus/GPa	Poisson's ratio
41.07	6.958	15.981	30.585	0.230	11.098	6.342	0.26

When  $RMFI < 1.0$ , the unit is under a safe state.

When  $RMFI = 1.0$ , the unit is under a critical state.

When  $RMFI > 1.0$ , the unit is under a failure state.

In this paper,  $RMFI$  (*rock mass failure index*) is employed to characterize the failure degree of the water-resistant strata, and it is also used as the energy criterion for the instability of the water-resistant strata. From formula (17), it can be seen that  $RMFI$  (*rock mass failure index*) corresponds to the stress state of the rock mass unit, and the greater the  $RMFI$  (*rock mass failure index*) is, the greater the failure degree of the rock mass unit is. Therefore, if the stress state of each element of the rock mass is acquired,  $RMFI$  (*rock mass failure index*) of the rock mass unit can be determined, and the instability and failure state of the water-resistant strata can be judged.

### 3. Stability Analysis of Water-Resistant Strata Based on $RMFI$ (*Rock Mass Failure Index*)

After the excavation of tunnel in karst areas, every rock mass unit is under the specific stress state. The whole compressive strength and tensile strength of rock mass are definite value. Then, the failure degree of each rock mass unit is corresponding to the stress state. Thus the numerical simulation method  $Flac^{3D}$  software can be applied, and the instability discrimination program of water-resistant strata based on releasable elastic strain energy  $U^e$  and  $RMFI$  (*rock mass failure index*) is compiled by FISH programming language in  $Flac^{3D}$  software. FISH is an array programming language that combines the functional programming with the execution of imperative (procedural) programming. So in the article FISH programming language was used which is embedded to  $Flac^{3D}$  software. In this way, we can gain distribution nephogram of releasable elastic strain energy  $U^e$  and  $RMFI$  (*rock mass failure index*), and  $RMFI$  (*rock mass failure index*) of every point in rock mass can be shown. The area of  $RMFI > 1.0$  indicates rock mass failure zone.

**3.1. Modeling.** Qiyueshan Tunnel of Liwan highway is selected as the background engineering in this paper. Rock mass mechanical parameters of section GK2480 are shown in Table 1. The karst cave is set at the top of the tunnel. Lateral pressure coefficient  $\lambda = 1.5$ , cavern spacing  $L = 3$  m, depth-span ratio of karst cave  $R = 1.0$  (circular), karst water pressure  $P = 1.0$  MPa, and setting the karst cave span  $D = 4$  m, 8 m, 12 m, 16 m, 20 m.

The karst tunnel model is taken as a plane strain model, which is taken as 1 m in longitudinal direction to calculate and analyze. Tunnel span  $d = 11.0$  m, clearance height  $h = 5.5$  m, and the model height is 85 m, which is 10 times as high as the tunnel height. The distance between the bottom of the tunnel and the bottom boundary of the model is 39.5 m. The distance

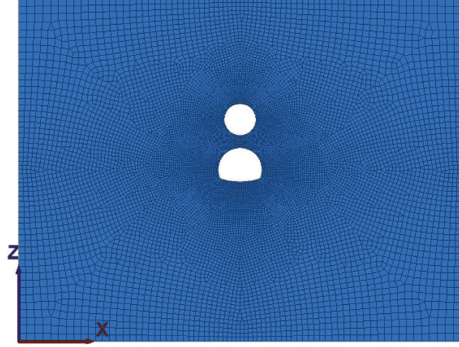


FIGURE 2: Model meshing diagram.

between the top of the tunnel and the upper boundary of the model is 37 m, and the tunnel depth is 307 m. Lateral stress is applied on the left and right boundary of the model, and the displacement constraint is applied at the bottom of the model. The load of upper rock mass is converted into uniform load and applied to the upper boundary of the model. The cave is considered as the mechanics model of the empty field [19]. Mesh generation of the model is shown in Figure 2, and the positions of the monitoring points are shown in Figure 3.

**3.2. Elastic Strain Energy's Distribution Characteristics Analysis of Water-Resistant Strata in Karst Tunnel.** The display program of the rock mass releasable elastic strain energy  $U^e$  is written in FISH programming language, and its distribution nephogram is shown in Figures 4 and 5.

The releasable elastic strain energy values at each monitoring point of the water-resistant strata under different cave spans are shown in Table 2.

The distribution curves of the releasable elastic strain energy and the minimum principal stress at the monitoring points of the water-resistant strata under different spans are shown in Figure 6.

It can be seen from Figure 6(a) that the elastic strain energy increases with the span  $D$  at each monitoring point (except the 1st unit at the bottom of the cave). When  $D = 4$  m and  $D = 8$  m, the releasable elastic strain energy is mainly distributed at the bottom of the cave ( $D = 4$  m,  $U^e = 0.088$  MJ/m<sup>3</sup>). As the span  $D$  increases, the releasable elastic strain energy is gradually transferred to the top of the tunnel, which is about 0.141 MJ/m<sup>3</sup>. The minimum principal stress distribution curve Figure 6(b) shows that water-resistant strata is under compression integrally, and the minimum principal stress at the top of the tunnel is the lowest. The amplification of minimum principal stress is only 20% with the increasing of the cave span. The triaxial test results of limestone show that the elastic energy storage capacity limit



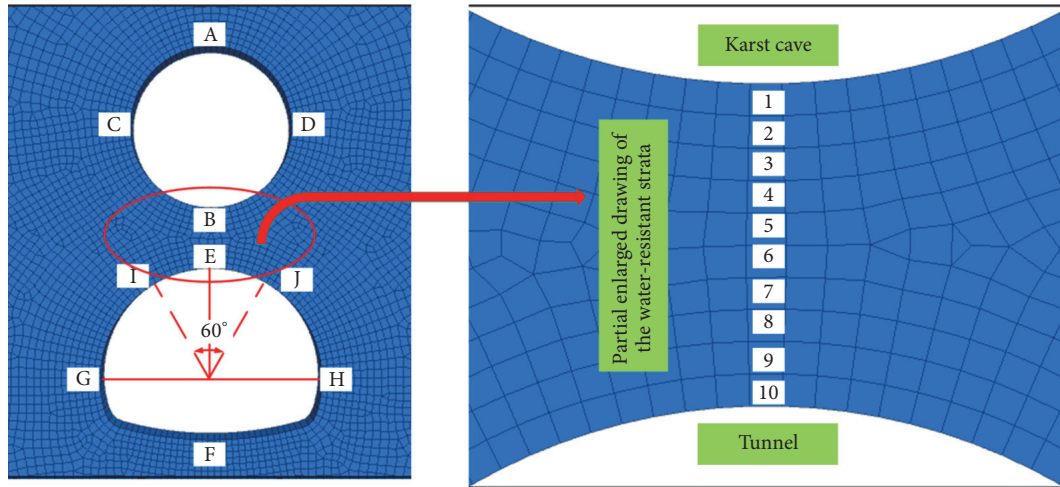
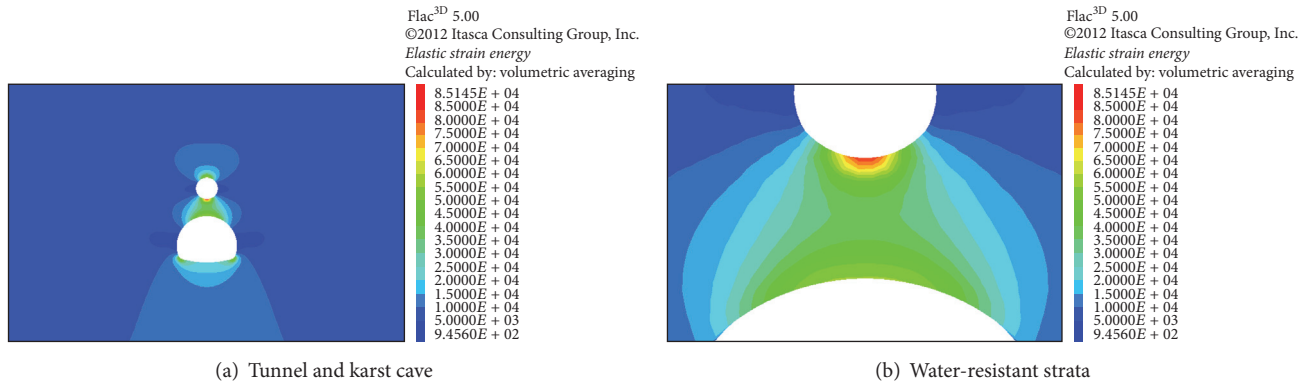
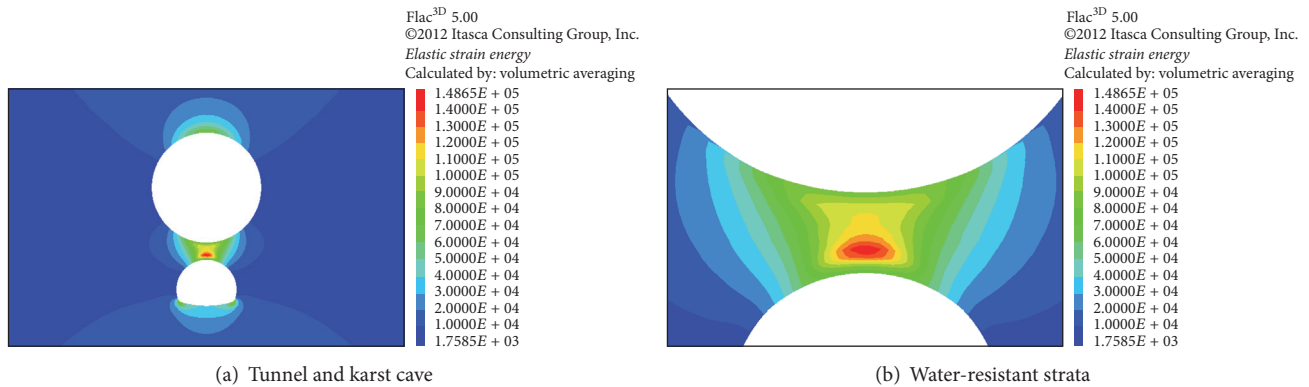


FIGURE 3: Layout of monitoring points.

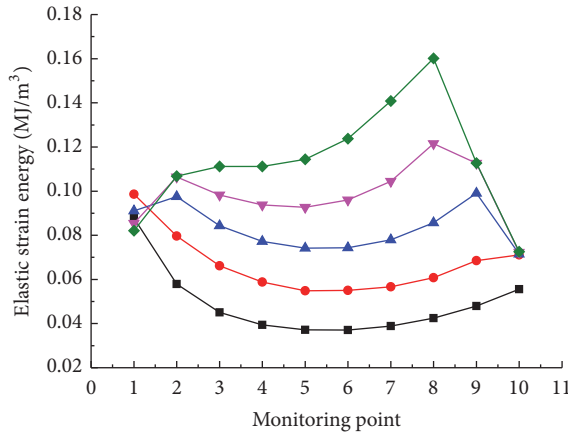
FIGURE 4:  $D = 4$  m releasable elastic strain energy distribution of the rock mass ( $\text{J}/\text{m}^3$ ).FIGURE 5:  $D = 20$  m releasable elastic strain energy distribution of surrounding rock ( $\text{J}/\text{m}^3$ ).

of the tunnel is proportional to the minimum principal stress [20, 21], and it is low at the top of the tunnel. Nevertheless, the releasable elastic strain energy is larger than other locations ( $D > 8$  m) at the top of the tunnel. It increases by 281% with the increasing tunnel span  $D$  at the top of the tunnel, which indicates that failure is prone to occur for the rock mass at the top of the tunnel and the damage will be severe.

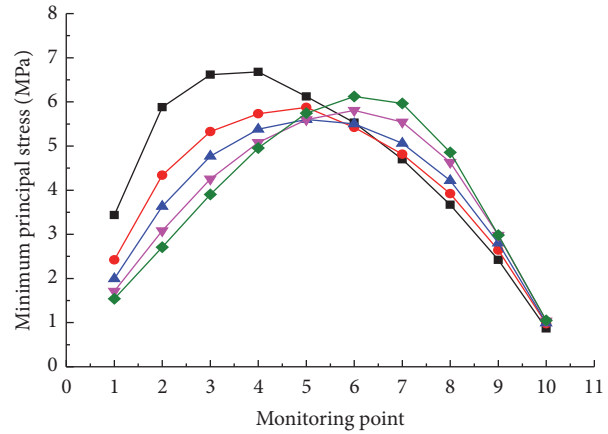
**3.3. Distribution Characteristics Analysis of RMFI for Water-Resistant Strata in Karst Tunnel.** FISH programming language was employed to write the RMFI display program, and its distribution nephogram was shown in Figure 7. To observe the scope of the area of the water-resistant strata, we can set it with conditional statement and the simulation approach is as follows: if  $\text{RMFI} < 1.0$ , the RMFI is set to 0. If  $\text{RMFI} > 1.0$ , the

TABLE 2: Releasable elastic strain energy at each monitoring point of the water-resistant strata under different cave spans (MJ/m<sup>3</sup>).

Karst cave span $D/m$	Monitoring point position									
	1	2	3	4	5	6	7	8	9	10
4	0.088	0.058	0.045	0.039	0.037	0.037	0.039	0.042	0.048	0.056
8	0.099	0.080	0.066	0.059	0.055	0.055	0.057	0.061	0.068	0.071
12	0.091	0.097	0.084	0.077	0.074	0.074	0.078	0.086	0.099	0.071
16	0.085	0.106	0.098	0.094	0.093	0.096	0.104	0.122	0.113	0.072
20	0.082	0.107	0.111	0.111	0.114	0.124	0.141	0.160	0.113	0.073



(a) Releasable elastic strain energy distribution curve



(b) Minimum principal stress distribution curve

FIGURE 6: Releasable elastic strain energy and minimum principal stress distribution curve at different spanners.

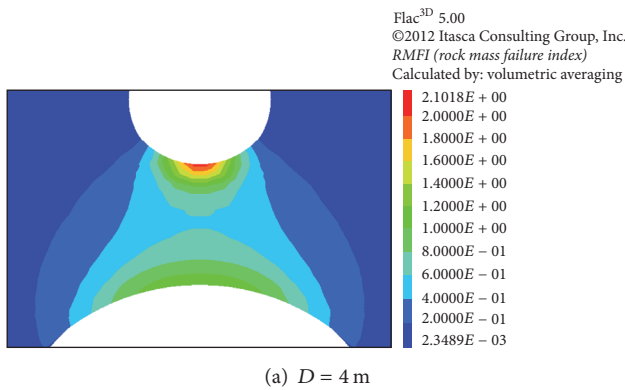
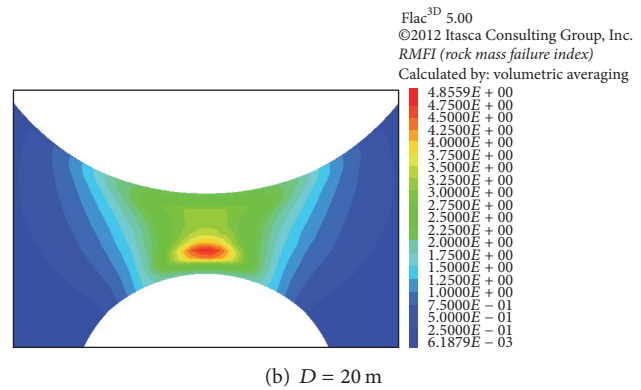
(a)  $D = 4$  m(b)  $D = 20$  m

FIGURE 7: Distribution of surrounding rock RMFI.

RMFI specific values are displayed normally, and  $RMFI > 1.0$  is the rock damage area as shown in Figure 8.

The RMFI values at the monitoring points of the water-resistant strata under different span are shown in Table 3.

The distribution curves of RMFI at each monitoring point of the water-resistant strata under different cave spans are shown in Figure 9.

It can be seen from Table 3 and Figure 9, when  $D = 4$  m, the RMFI is 2.196 at the bottom of karst cave. When  $D > 4$  m,

the RMFI at the bottom of karst cave decreases with the increasing of the karst cave span  $D$ , and the RMFI decreases from 2.196 to 1.981. The RMFI at other monitoring points of the water-resistant strata increases with the increasing of the karst cave span  $D$ . When  $D = 4$  m, failure occur at the bottom of the karst cave while other locations are safe and stable. When  $D = 8$  m, the large value of RMFI mainly distribute near the bottom of the karst cave ( $RMFI = 2.614$ ). When  $D > 8$  m, the large value of RMFI gradually shift to the

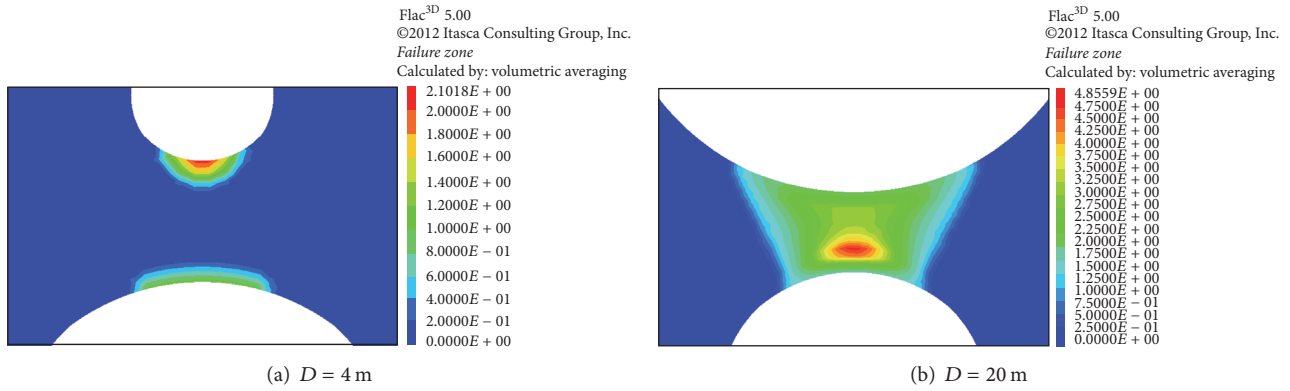


FIGURE 8: Distribution of surrounding rock failure zone.

TABLE 3: RMFI values of each monitoring point of water-resistant strata under different cave spans.

Karst cave span $D$ /m	Monitoring points' position									
	1	2	3	4	5	6	7	8	9	10
4	2.196	1.172	0.794	0.645	0.594	0.595	0.645	0.739	0.888	1.101
8	2.614	1.900	1.435	1.199	1.078	1.087	1.137	1.269	1.515	1.596
12	2.318	2.574	2.072	1.812	1.705	1.713	1.838	2.122	2.633	1.608
16	2.105	2.934	2.604	2.426	2.385	2.515	2.854	3.583	3.191	1.636
20	1.981	2.947	3.137	3.135	3.273	3.680	4.472	5.420	3.196	1.644

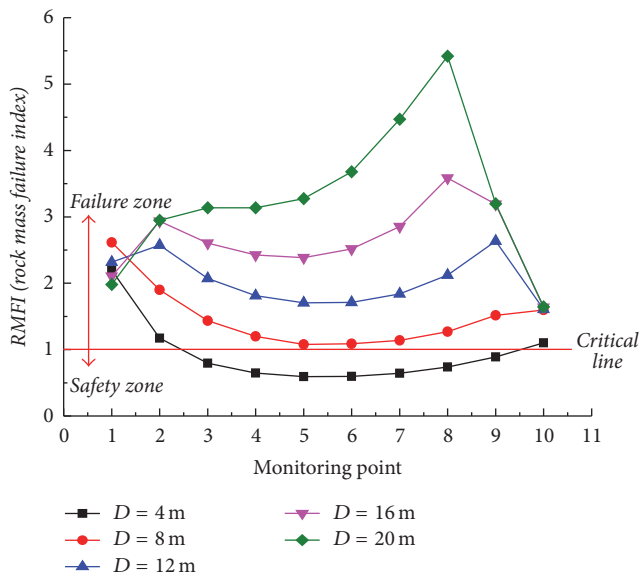


FIGURE 9: RMFI distribution curves of each monitoring points of water-resistant strata under different cave spans.

top of the tunnel with the increasing of the karst cave span. When  $D = 12$  m (the tunnel span  $d$ ), the large value of RMFI transfer to the top of the tunnel, and the failure zone of the water-resistant strata penetrates. When  $D = 20$  m ( $D > 2d$ ), the RMFI at the top of the tunnel rises to 5.420 and at the bottom of the karst cave decreases to 1.981. The top of the tunnel is damaged severely compared with other locations.

The paper takes some influence factors of the karst cave span  $D$  as an example and analyzes the stability of the water-resistant strata and the distribution law of damage area, which is based on releasable elastic strain energy and RMFI (rock mass failure index). It is intuitive and objective unification. The releasable elastic strain energy and RMFI (rock mass failure index) of each point of the rock mass can be obtained quantitatively, and the failure zone of water-resistant strata can be observed directly. If the critical distance of failure zone of water-resistant strata is defined as safety thickness [2], combined with the RMFI display program and adjusting the distance between tunnel and the karst cave continuously, the safety thickness of the water-resistant strata can be determined vividly.

#### 4. Engineering Application

Yichang-Wanzhou Railway Dazhiping tunnel is a two-lane tunnel. There is a water-rich karst cave at mileage DK137 + 768.5~DK137 + 783.6. The internal water pressure is 0.73~0.89 MPa. The cave span is 7.7~9.2 m, and the cave height is 5.5~7.8 m. The longitudinal span along the axial direction of the tunnel is about 13~15 m. The relationship of the location between the cave and the tunnel is shown in Figure 10.

The karst cave can be simplified as an ellipse, with the major axis 8.45 m and the short axis 6.65 m. The depth of the tunnel is 110 m. Rock parameters are selected from the limestone test data obtained by Wang et al. [4]. The tensile strength and compressive strength of rock mass is 0.570 MPa and 7.081 MPa, respectively, and the lateral pressure coefficient is 1.3. The density of rock mass is 26.5 kN/m<sup>3</sup>. The

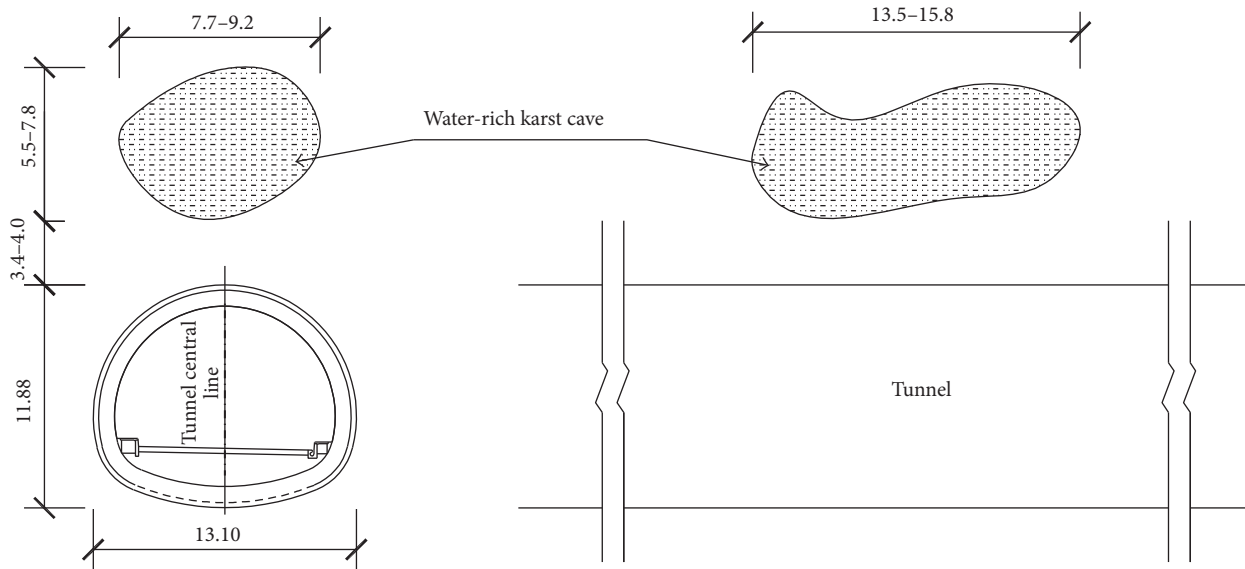


FIGURE 10: Location relationship diagram between Dazhiping tunnel and karst cave in DK137 + 768.5~DK137 + 783.6.

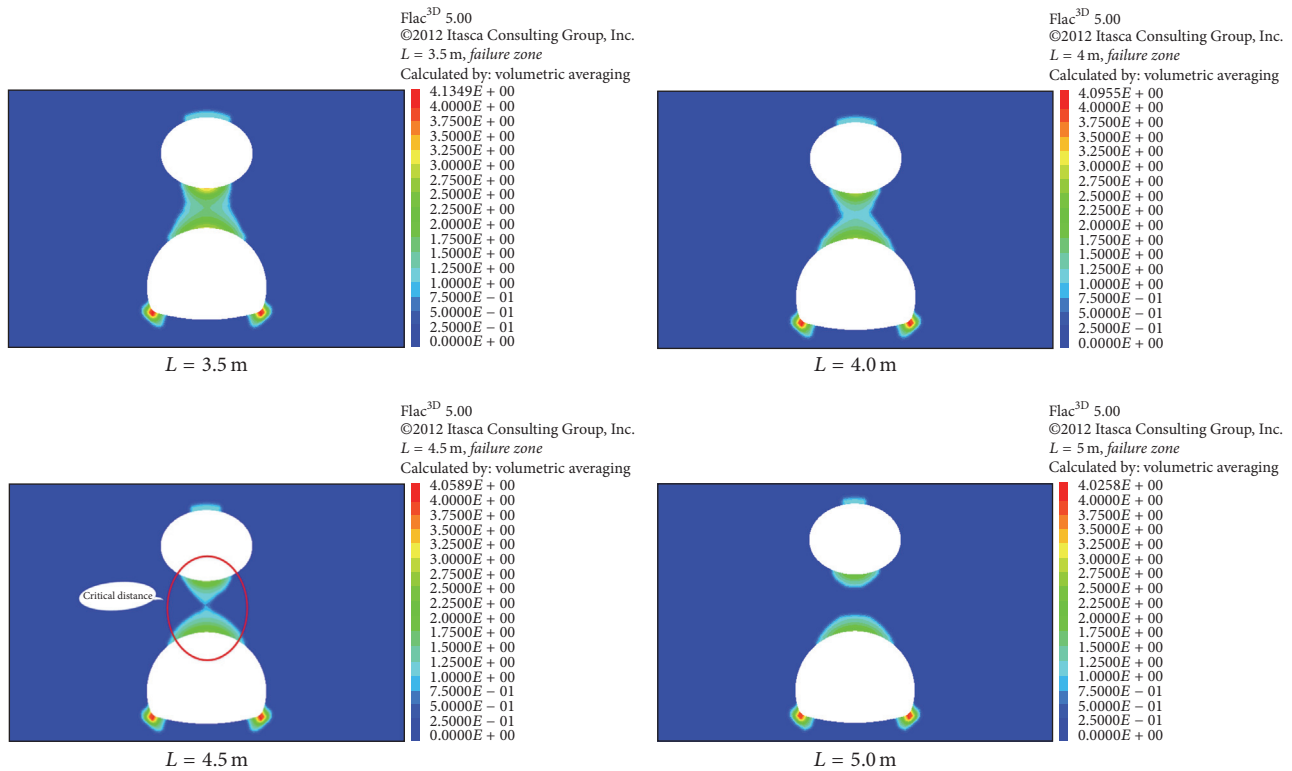


FIGURE 11: Destruction zone of water-resistant strata with the karst cave space changing in Dazhiping tunnel at the section DK137 + 768.5~DK137 + 783.6.

bulk modulus is 17.371 GPa. Shear modulus is 7.808 GPa, and Poisson ratio is 0.27. We adjust the distance between the karst cave and the tunnel constantly, until the critical location of the failure zone of water-resistant strata was found (critical contact position where  $RMFI > 1.0$ ). The distance between the top of the tunnel and the bottom of the karst cave is the safe distance (Figure 11).

Figure 11 reveals that the safety thickness of water-resistant strata is about 4.5 m in Dazhiping tunnel, and the result is similar to the calculation result (4.3 m) which is obtained by Guo [5] through the Schwarz alternating method and Griffith strength criterion. During the construction process, we have explored that the distance between lower boundary of karst cave and the top of tunnel is 3.4 m~4 m.



Thus, the water-resistant strata are instable. In actual construction, the pregrouting and advanced pipe roof support is employed, and finally the area influenced by the karst cave is accomplished successfully.

## 5. Conclusions

- (1) The energy instability criterion of water-resistant strata based on releasable elastic strain energy  $U^e$  is established and RMFI (rock mass failure index) is defined. It is employed as energy criterion to characterize the damage degree of water-resistant strata. If  $RMFI < 1.0$ , the rock mass is stable. If  $RMFI = 1.0$ , the rock mass is in the critical state. If  $RMFI > 1.0$ , the rock mass is instable.
- (2) The releasable elastic strain energy  $U^e$  and RMFI program was compiled by FISH programming language of Flac<sup>3D</sup> software. Combined with this program, Flac<sup>3D</sup> software to analyze the influence of concealed karst cave  $D$  on the failure zone is applied.
- (3) Combined with the releasable elastic strain energy  $U^e$  and RMFI defined in this paper, safety thickness of water-resistant strata in Dazhiping tunnel is determined by the RMFI instability discrimination program. The result is close to the practical engineering. Therefore, this method can be used as a tool for confirming other prediction methods or as a basis for engineering decision.

## Competing Interests

The authors declare that there is no conflict of interests regarding the publication of this paper.

## Acknowledgments

This study was supported by the State Key Development Program for Basic Research of China (Grant no. 2013CB036003), National Natural Science Fund Project (Grant no. 51408054), the Ministry of Education Doctoral Fund (20130205110004), and the Fundamental Research Funds for the Central Universities (Grant nos. 310821163115 and 310828161004).

## References

- [1] M. Zhang, *Construction Technology of Karst Tunnel in Yiwan Railway*, Science Press, Beijing, China, 2010.
- [2] X. Cao, *Study on safe thickness between tunnel and karst cave in karst region [M.S. thesis]*, Beijing Jiaotong University, 2010.
- [3] L. Li, T. Lei, S. Li et al., "Risk assessment of water inrush in karst tunnels and software development," *Arabian Journal of Geosciences*, vol. 8, no. 4, pp. 1843–1854, 2015.
- [4] Y. Wang, C.-S. Qiao, C.-H. Sun, and K.-Y. Liu, "Forecasting model of safe thickness for roof of karst cave tunnel based on support vector machines," *Rock and Soil Mechanics*, vol. 27, no. 6, pp. 1000–1004, 2006.
- [5] J. Q. Guo, *Study on against-inrush thickness and waterburst mechanism of karst tunnel [Ph.D. thesis]*, Beijing Jiaotong University, 2011.
- [6] S. Yin, S. Wang, and Q. Wu, "Water inrush patterns and theoretic criteria of karstic collapse columns," *Chinese Journal of Rock Mechanics and Engineering*, vol. 23, no. 6, pp. 964–968, 2004.
- [7] L. P. Li, *Study on catastrophe evolution mechanism of karst water inrush and its engineering application of high risk karst tunnel [Ph.D. thesis]*, Shandong University, 2009.
- [8] D. L. Zhou and J. F. Zou, "Safe thickness of floor of forked tunnel in karst areas," *Journal of Central South University (Science and Technology)*, vol. 46, no. 5, pp. 1886–1892, 2015.
- [9] B. Chen, C. Gu, T. Bao, B. Wu, and H. Su, "Failure analysis method of concrete arch dam based on elastic strain energy criterion," *Engineering Failure Analysis*, vol. 60, pp. 363–373, 2016.
- [10] B. Li and H. Y. Wang, "Numerical analysis of the influence of karst cave on deformation and stress of surrounding rock in the bottom," *Highway*, no. 5, pp. 223–226, 2016.
- [11] Y. R. Zheng, *Stability Analysis and Design Theory of Underground Engineering Surrounding Rock*, People Traffic Press, Beijing, China, 2012.
- [12] C.-Q. Zhang, H. Zhou, and X.-T. Feng, "Stability assessment of rockmass engineering based on failure approach index," *Rock and Soil Mechanics*, vol. 28, no. 5, pp. 888–894, 2007.
- [13] H. Xie, Y. Ju, L. Li, and R. Peng, "Energy mechanism of deformation and failure of rock masses," *Chinese Journal of Rock Mechanics and Engineering*, vol. 27, no. 9, pp. 1729–1740, 2008.
- [14] H.-P. Xie, Y. Ju, and L.-Y. Li, "Criteria for strength and structural failure of rocks based on energy dissipation and energy release principles," *Chinese Journal of Rock Mechanics and Engineering*, vol. 24, no. 17, pp. 3003–3010, 2005.
- [15] H. P. Xie, R. D. Peng, H. W. Zhou, and Y. Ju, "Research progress of rock strength theory based on fracture mechanics and damage mechanics," *Progress in Natural Science*, vol. 14, no. 10, pp. 7–13, 2004.
- [16] W. Wu, G. Jiang, S. Huang, and C. J. Leo, "Vertical dynamic response of pile embedded in layered transversely isotropic soil," *Mathematical Problems in Engineering*, vol. 2014, Article ID 126916, 12 pages, 2014.
- [17] S. P. Singh, "Burst energy release index," *Rock Mechanics and Rock Engineering*, vol. 21, no. 2, pp. 149–155, 1988.
- [18] M. S. Dehkordi, H. A. Lazemi, and K. Shahriar, "Application of the strain energy ratio and the equivalent thrust per cutter to predict the penetration rate of TBM, case study: Karaj-Tehran water conveyance tunnel of Iran," *Arabian Journal of Geosciences*, vol. 8, no. 7, pp. 4833–4842, 2014.
- [19] Z. P. Song, *Research on the influence of concealed karst caverns upon the stability of tunnels and its support structure [Ph.D. thesis]*, Xi'an University of Technology, 2006.
- [20] J. Guo, X. Liu, and C. Qiao, "Experimental study of mechanical properties and energy mechanism of karst limestone under natural and saturated states," *Chinese Journal of Rock Mechanics and Engineering*, vol. 33, no. 2, pp. 296–308, 2014.
- [21] L.-M. Zhang, S. Gao, and Z.-Q. Wang, "Experimental study of energy evolution of limestone under loading and unloading conditions," *Rock and Soil Mechanics*, vol. 34, no. 11, pp. 3071–3076, 2013.

